Science Advances

AAAS

advances.sciencemag.org/cgi/content/full/3/12/eaao1497/DC1

Supplementary Materials for

Multivalent ions induce lateral structural inhomogeneities in polyelectrolyte brushes

Jing Yu, Nicholas E. Jackson, Xin Xu, Blair K. Brettmann, Marina Ruths, Juan J. de Pablo, Matthew Tirrell

Published 8 December 2017, *Sci. Adv.* **3**, eaao1497 (2017)
DOI: 10.1126/sciadv.aao1497

This PDF file includes:

- fig. S14. Polymer density plots for the polydisperse simulation using conditions corresponding to Fig. 3B.
- fig. S15. Polymer density plots for the polydisperse simulation using conditions corresponding to Fig. 3C.
- fig. S16. Polymer density plots for the polydisperse simulation using conditions corresponding to Fig. 3D.
- fig. S17. Polymer density plots for the polydisperse simulation using conditions corresponding to Fig. 6A.
- fig. S18. Polymer density plots for the polydisperse simulation using conditions corresponding to Fig. 6B.
- fig. S19. Polymer density plots for the polydisperse simulation using conditions corresponding to Fig. 6C.
- fig. S20. Polymer density plots for the polydisperse simulation using conditions corresponding to Fig. 6D.
- Representative large-scale atomic/molecular massively parallel simulator input (used to generate data in Fig. 6C).

AFM imaging in solution

AFM images were acquired with tips (CSC17/Cr-Au, MikroMasch) that typically had a radius of curvature of 20–30 nm as established for several tips from the same batch through reverse imaging of a calibration sample (TGT01, MicroMasch).

AFM imaging in solution was performed using a glass liquid cell (model MTFML, Bruker) with a syringe port for injecting liquids (volume ca. 0.1 mL) and an outlet for excess liquid. The waiting time between the first exposure of a dry PSS layer to water or electrolyte solution in the liquid cell and the start of the imaging was 10–15 min. Brush samples used for IPA/water measurements were soaked in DI water for 10 min and then air dried before mounting them in the liquid cell and introducing the solution. When changing to another solution, the sample was first taken out and rinsed with water and air dried, then placed back under the liquid cell and the new solution introduced. The liquid cell was rinsed with large amount of water and ethanol and air dried between each solution. To ensure statistically significant surface sampling, several different regions on each sample were scanned, showing the same qualitative structure at a given condition.

Figure S1 shows the formation of lateral structures with $Y(NO_3)_3$ in systems that did not contain monovalent counterions. Structures were observed at a lower $Y(NO_3)_3$ content (0.01 M) than when Na^+ was present in the solution (cf. Fig. 1B at 0.1 M $Y(NO_3)_3$).

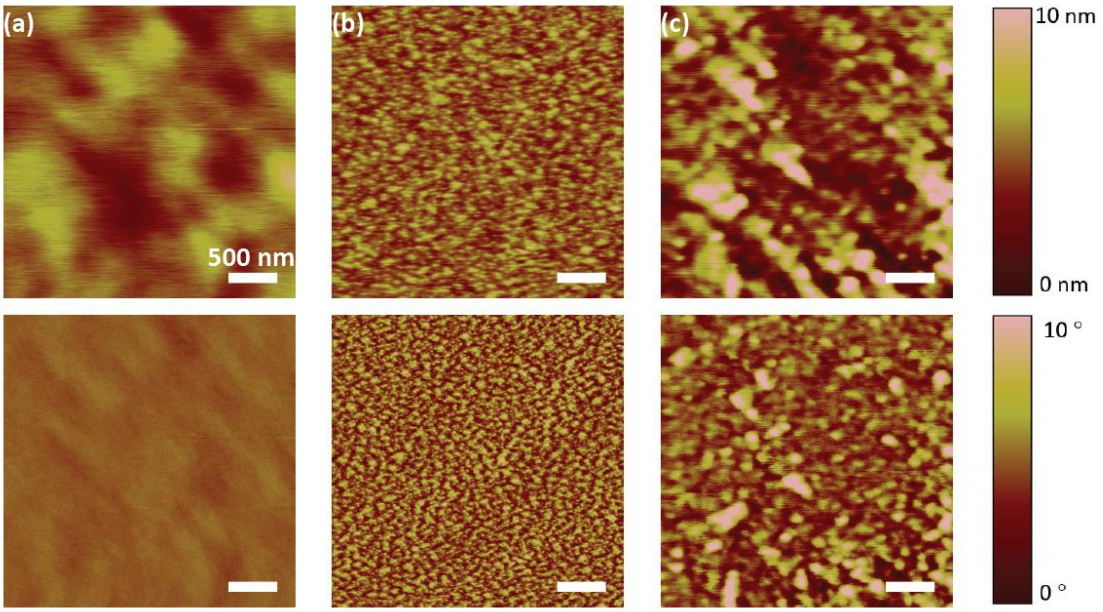

fig. S1. AFM images of PSS brush layers in the absence and presence of multivalent ions. Tapping mode height (top) and phase images (bottom). (**A**) No distinct features were seen in deionized water (no added salt). (**B**) Lateral structures formed in 0.01 mM $Y(NO_3)_3$ solution (also used as Fig. 2a). (**C**) 1 mM $Y(NO_3)_3$. Scan size 3 μm × 3 μm.

Polymer and Ion distributions at low-grafting densities (Main Text - Fig 3)

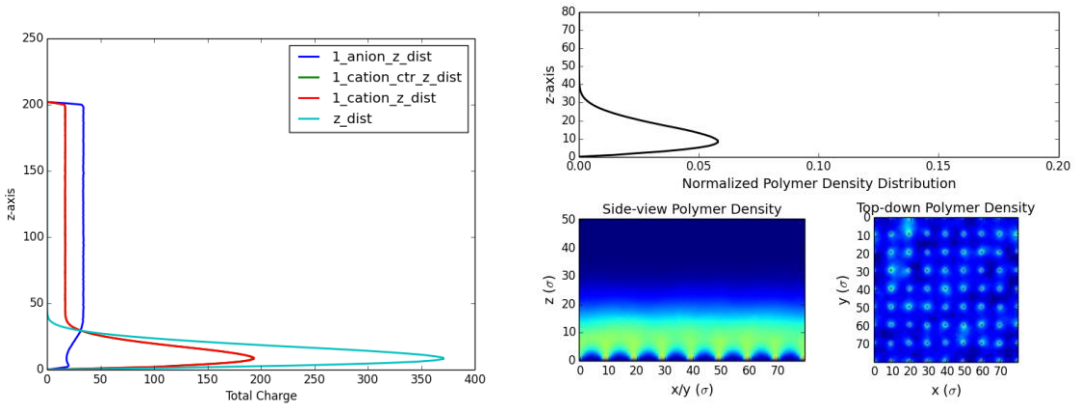

fig. S2. Charge distribution and polymer density plots corresponding to the data presented in Fig. 3A. (left) charge distribution and (right) polymer density plots corresponding to the data presented in the main text Figure 3A.

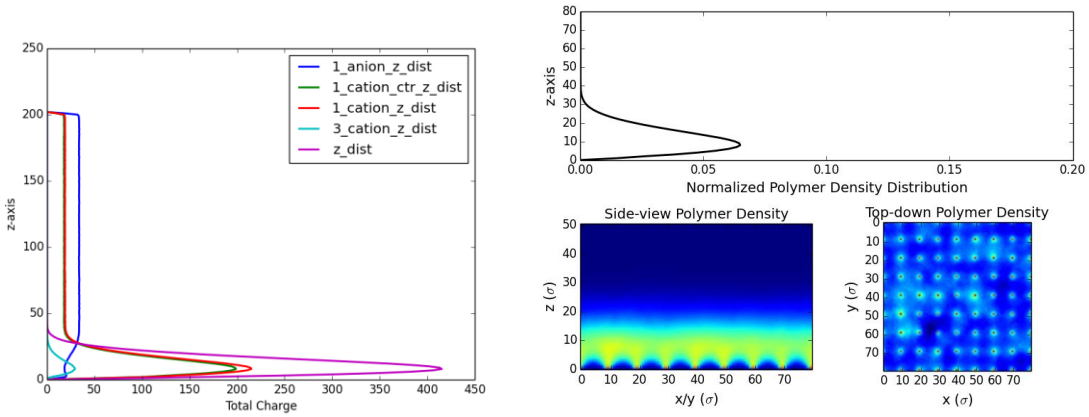

fig. S3. Charge distribution and polymer density plots corresponding to the data presented in Fig. 3B. (left) charge distribution and (right) polymer density plots corresponding to the data presented in the main text Figure 3B.

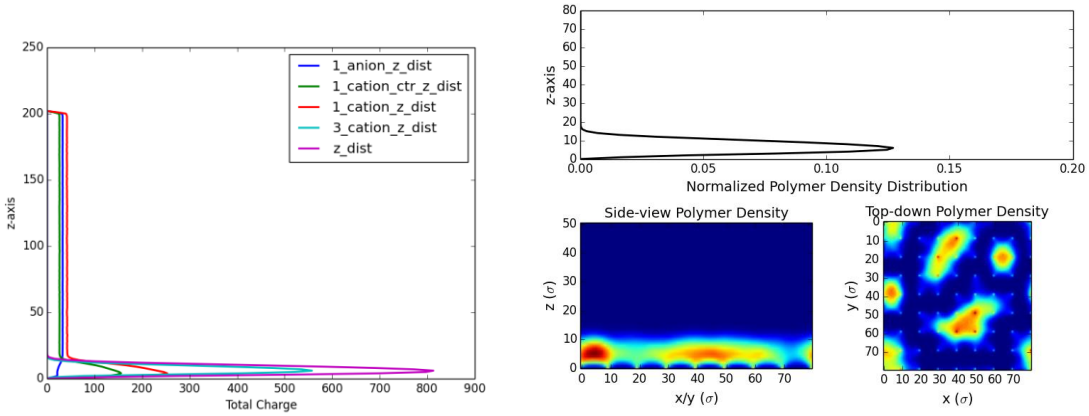

fig. S4. Charge distribution and polymer density plots corresponding to the data presented in Fig. 3C. (left) charge distribution and (right) polymer density plots corresponding to the data presented in the main text Figure 3C.

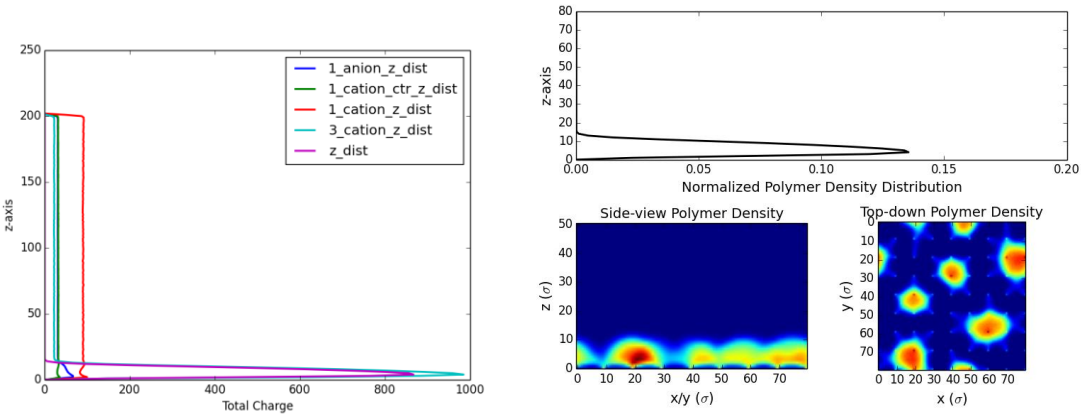

fig. S5. Charge distribution and polymer density plots corresponding to the data presented in Fig. 3D. (left) charge distribution and (right) polymer density plots corresponding to the data presented in the main text Figure 3D.

MD simulations of diffusion rates of trivalent counterions

In figure S6 we display the distribution of diffusion rates of multivalent ions from MD simulations of the data corresponding to Figure 3c of the main text. The results shown are for the collapsed brush and demonstrate that nearly 90% of counterions are essentially immobilized in the brush (very low diffusion rate) – moreover, for the majority of the fits of the diffusion constant, the linear region is never reached. Units of the diffusion coefficents are σ^2/τ, where τ is the characteristic timescale of the system in Lennard Jones units, and σ is the system length scale, corresponding to the size of a coarse-grained bead. To compute the diffusion coefficient, we utilize the 3-dimensional Einstein relation:

$$\langle \Delta r^2(t) \rangle = 6Dt$$

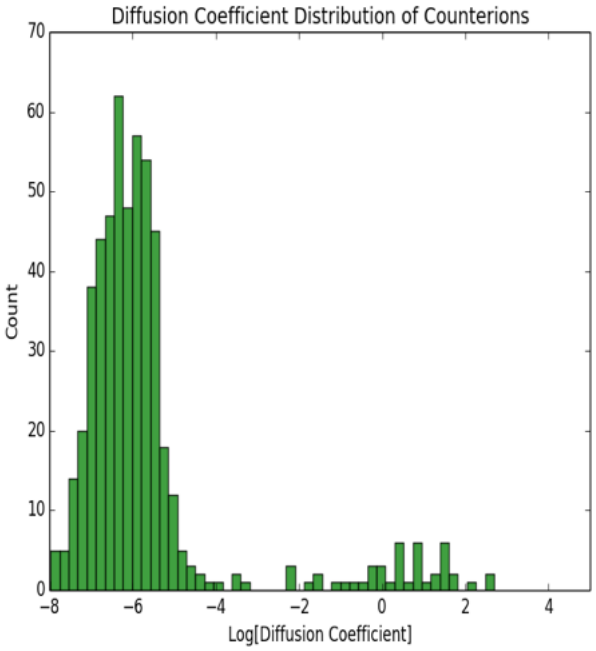

fig. S6. Distribution of diffusion rates of trivalent ions in the collapsed brush systems computed via the root-mean-squared distances as a function of time. Note that the *x*-axis is a log scale.

Neutron reflectivity measurement compared to simulation results

In figure S7 the neutron reflectivity (NR) data is compared to the polymer and ion distributions obtained from the coarse-grained MD simulations. It is evident that the MD results match the qualitative volume fraction profile determined from NR, reproducing the general shape, including the tail at large heights. Provided the factor of 10 molecular weight difference between MD and experiment, it is expected that the experimental NR tail is more substantial than that from MD.

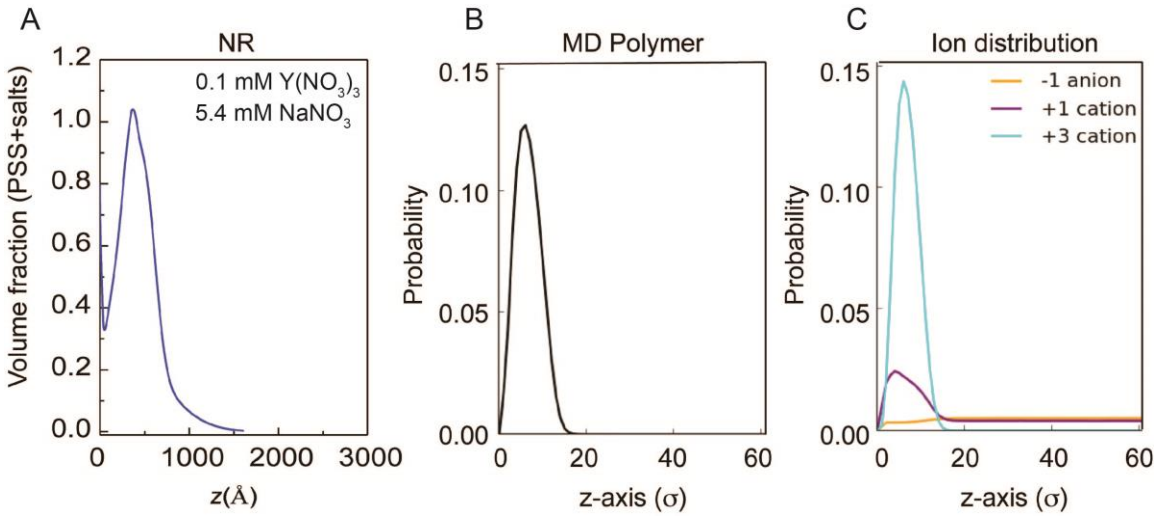

fig. S7. Distributions of polyelectrolytes and ions in a brush layer. (**A**) Volume fraction of the PSS polymer and counterions trapped in a PSS brush layer measured by neutron reflectivity (NR). (**B**) Distribution of the polyelectrolyte and (**C**) counter- and co-ions in the brush layer, from MD simulations, corresponding to the conditions of the main text Figure 3c.

Moreover, since NR cannot differentiate the relative distributions of ions within the brush, MD was used to examine the ratio of counterions at a moderate trivalent ion concentration just under the neutralization condition. The simulations clearly show that the multivalent cations are entirely localized within the brush volume, in addition to a small quantity of monovalent cations – this combination of available cations serves to effectively neutralize the total charge of the brush, with multivalent cations being preferentially condensed. The rest of the monovalent counterions not involved in brush neutralization are essentially uniformly distributed throughout the remainder of the simulation box.

The collapse of the brush layers in a poor solvent was studied as a function of IPA/water ratio. fig. S8 shows an example of height and phase images obtained in pure IPA, where a homogeneously collapsed layer formed, similarly to in 80% IPA (Fig. 5).

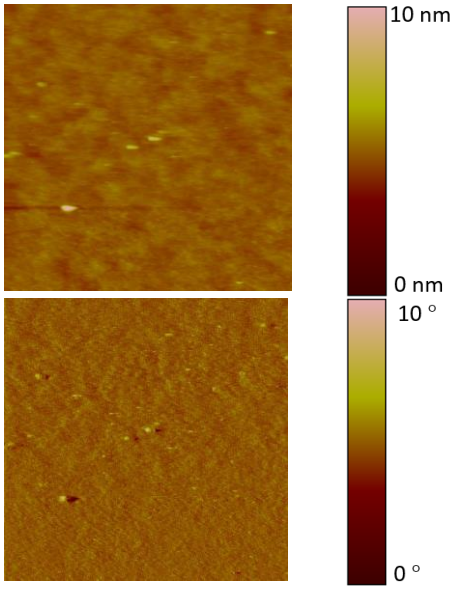

fig. S8. Collapsed PSS brush layer in poor solvent. Height (top) and phase (bottom) image of PSS brushes in 100% IPA. Scan size 3 μm × 3 μm.

<u>Polymer and Ion distributions at high-grafting densities (Main Text – Fig 6)</u>

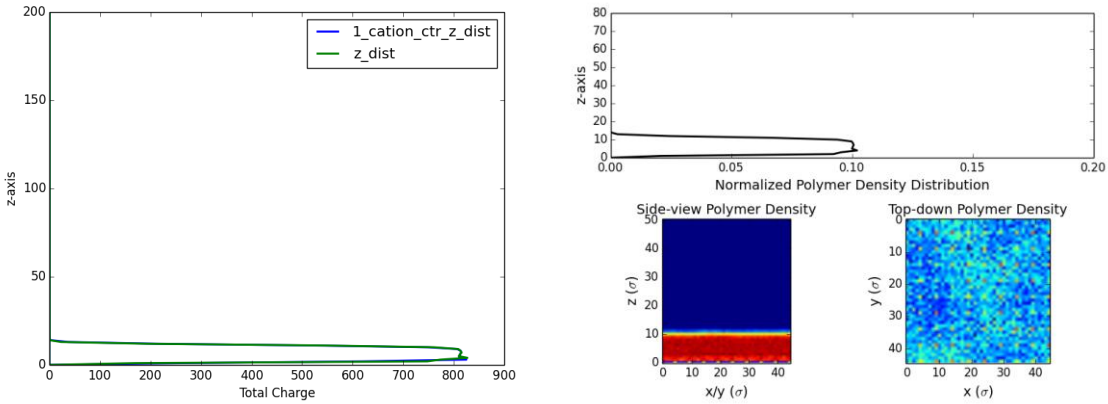

fig. S9. Charge distribution and polymer density plots corresponding to the data presented in Fig. 6A. (left) charge distribution and (right) polymer density plots corresponding to the data presented in the main text Figure 6A.

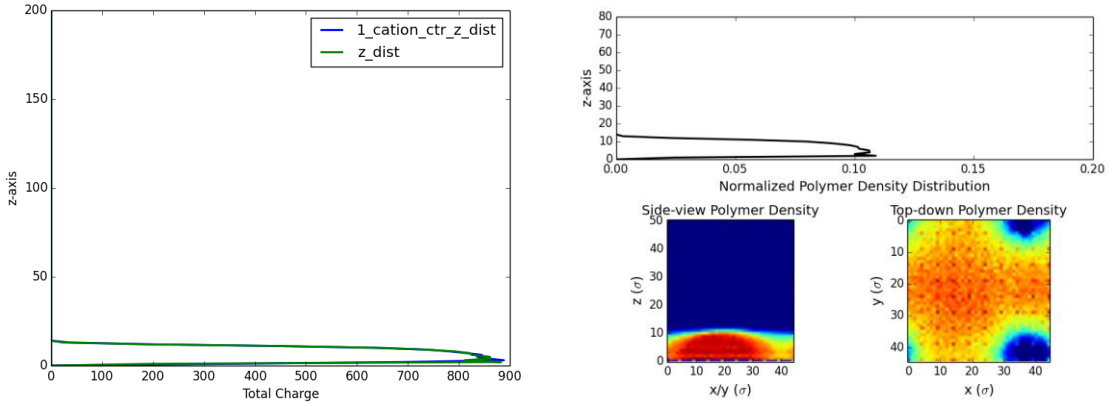

fig. S10. Charge distribution and polymer density plots corresponding to the data presented in Fig. 6B. (left) charge distribution and (right) polymer density plots corresponding to the data presented in the main text Figure 6B.

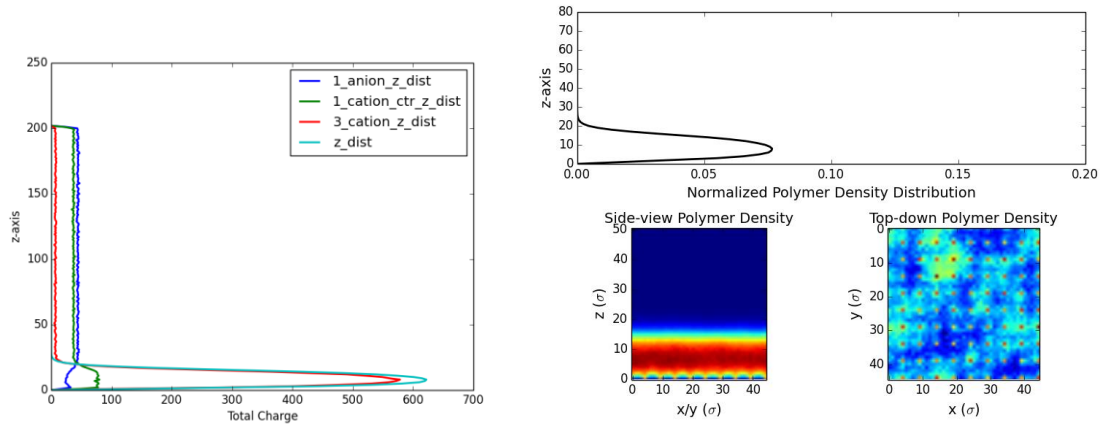

fig. S11. Charge distribution and polymer density plots corresponding to the data presented in Fig. 6C. (left) charge distribution and (right) polymer density plots corresponding to the data presented in the main text Figure 6C.

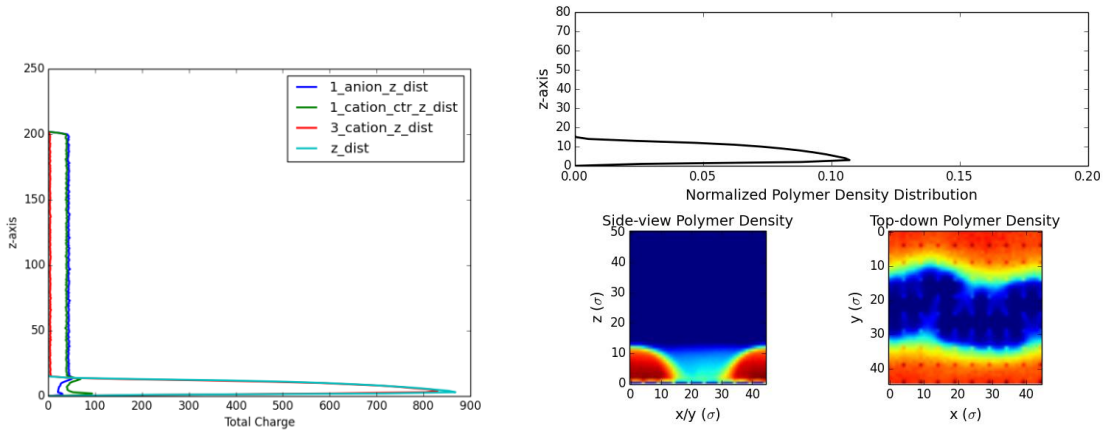

fig. S12. Charge distribution and polymer density plots corresponding to the data presented in Fig. 6D. (left) charge distribution and (right) polymer density plots corresponding to the data presented in the main text Figure 6D.

Polymer and Ion Simulations Incorporating Polydispersity

To explore the impact of polydispersity on brush morphology we have re-run the simulations of Fig. 3 and Fig. 6 from the main text using a bimodal distribution of polyelectrolyte chain lengths. Experimentally, the polydispersity for our system is anticipated to be 1.1–1.25. To test the impact of polydispersity on the observed brush morphologies, we considered the upper limit of the PDI (1.25), and randomly placed a 50/50 mixture of length 50 chains and length 150 chains for all simulation conditions. We note that the bimodal distribution of chains should serve to exaggerate any potential polydispersity induced effects, as the actual distribution function should be much smoother.

The primary conclusion of the polydisperse simulations is that for the 10 sigma grafting density, polydispersity has no noticeable effect on the morphologies. However, at 5 sigma, if there is a region with strongly mismatched molecular weight chains, one will see a depletion in the polymer density near the short MW chain region if the brush is collapsed. These surface heterogeneities are explained by the natural surface roughness induced by the molecular weight mismatches in the collapsed regime. Provided that our simulations consider the upper-limit of potential polydispersity, it is extremely unlikely that the polydispersity in the experimental system is solely capable of inducing the heterogeneities observed in the AFM images, though our simulations suggest that provided a confluence of conditions (including trivalent ions), polydispersity could certainly enhance the observed surface heterogeneities.

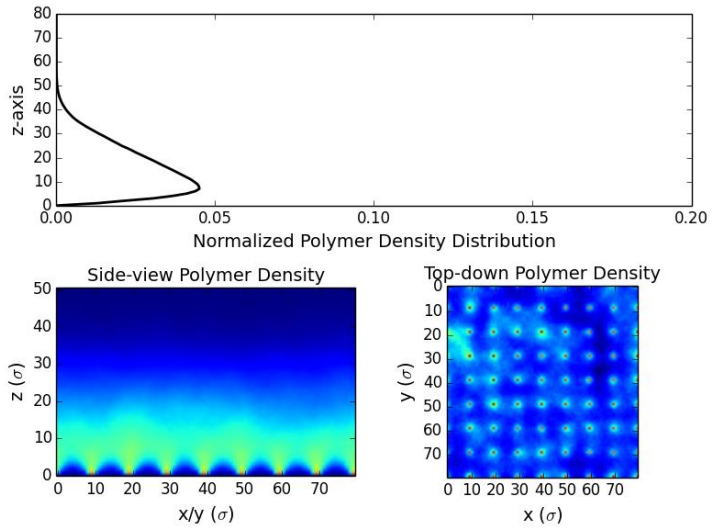

fig. S13. Polymer density plots for the polydisperse simulation using conditions corresponding to Fig. 3A.

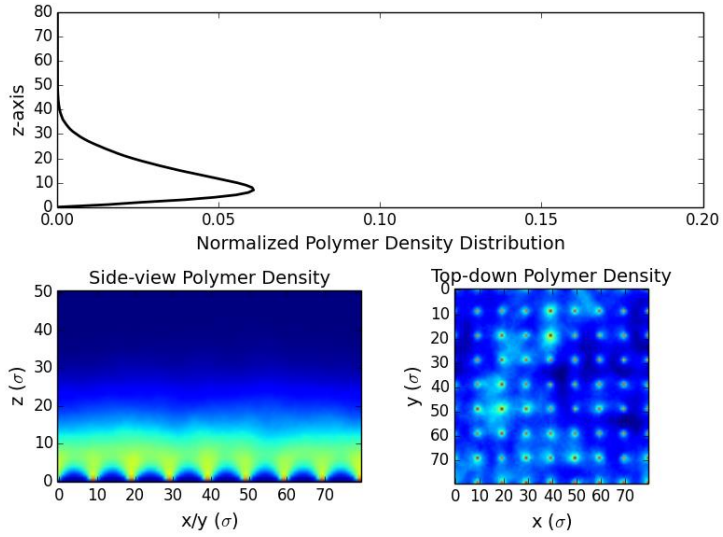

fig. S14. Polymer density plots for the polydisperse simulation using conditions corresponding to Fig. 3B.

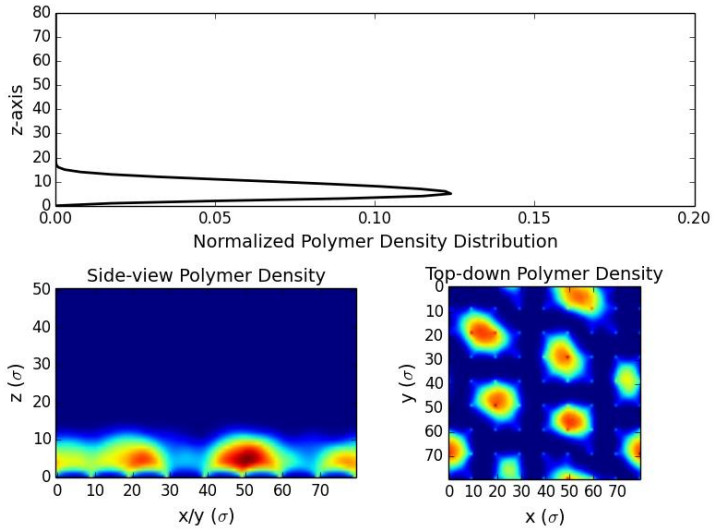

fig. S15. Polymer density plots for the polydisperse simulation using conditions corresponding to Fig. 3C.

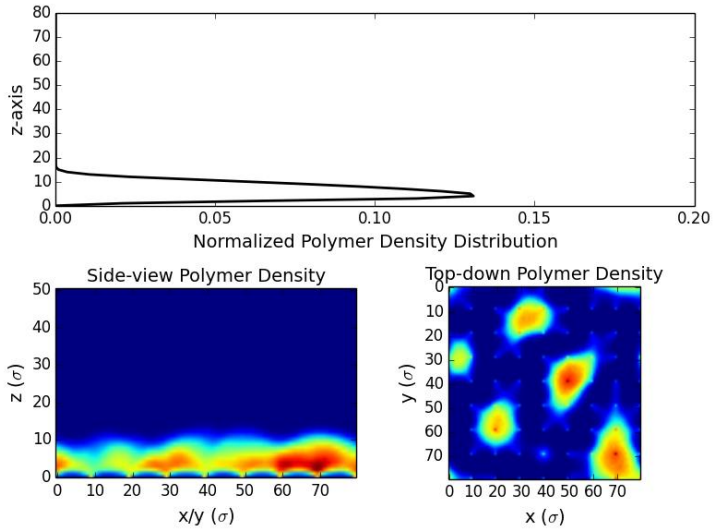

fig. S16. Polymer density plots for the polydisperse simulation using conditions corresponding to Fig. 3D.

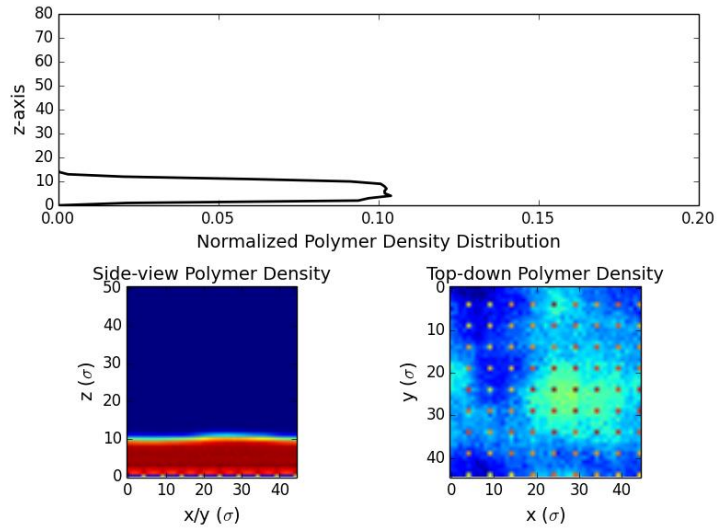

fig. S17. Polymer density plots for the polydisperse simulation using conditions corresponding to Fig. 6A.

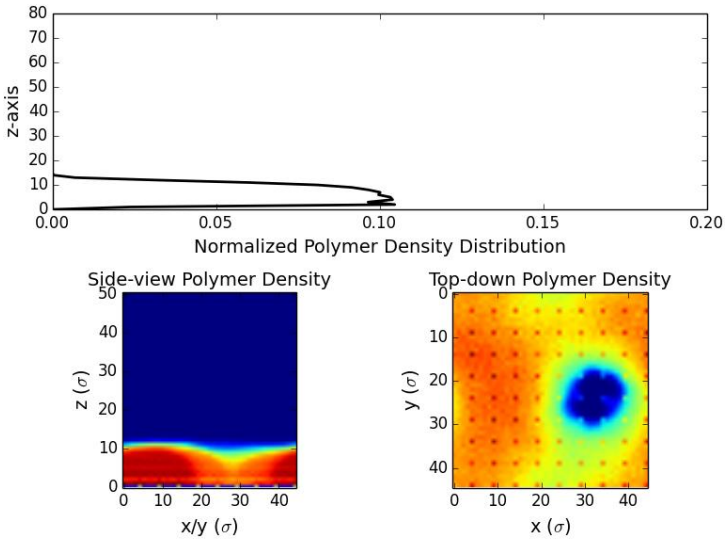

fig. S18. Polymer density plots for the polydisperse simulation using conditions corresponding to Fig. 6B.

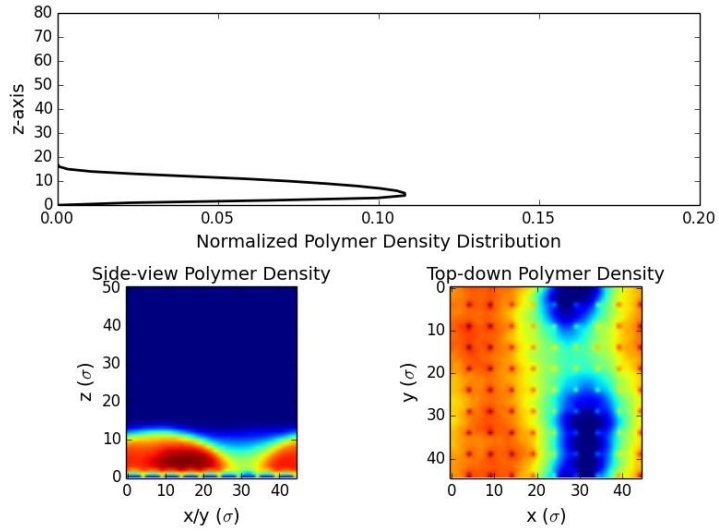

fig. S19. Polymer density plots for the polydisperse simulation using conditions corresponding to Fig. 6C.

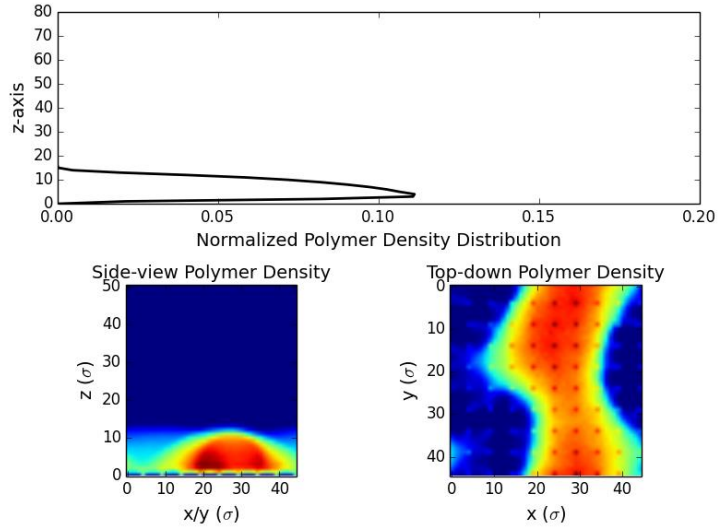

fig. S20. Polymer density plots for the polydisperse simulation using conditions corresponding to Fig. 6D.

Representative large-scale atomic/molecular massively parallel simulator input (used to generate data in Fig. 6C).

```
units           lj
atom_style      full
pair_style      lj/cut/coul/long 2.5 5.5
pair_modify     shift yes mix arithmetic
bond_style      fene
angle_style     cosine/delta
boundary        p p f
neighbor        0.5 bin
neigh_modify    every 1 delay 3 check yes one 10000
kspace_style    pppm   0.001
kspace_modify    slab   3.0
special_bonds   fene

#---------- Particle Definitions ----------
read_data "brush.data"

#Non-bonded interactions (pair-wise)
pair_coeff 1 1 0.0 1.0
pair_coeff 1 2 0.0 1.0
pair_coeff 1 3 0.0 1.0
pair_coeff 1 4 0.0 1.0
pair_coeff 1 5 0.0 1.0
pair_coeff 2 2 0.4 1.0
pair_coeff 2 3 0.4 1.0
pair_coeff 2 4 0.4 1.0
pair_coeff 2 5 0.4 1.0
pair_coeff 3 3 0.4 1.0
pair_coeff 3 4 0.4 1.0
pair_coeff 3 5 0.4 1.0
pair_coeff 4 4 0.4 1.0
pair_coeff 4 5 0.4 1.0
pair_coeff 5 5 0.4 1.0

#FENE Stretching Interactions
#bond_coeff bondtype k R0 epsilon sigma
bond_coeff 1 30.0 1.5 1.0 1.0

#Harmonic Angle Interaction
angle_coeff 1 1.0 180.0#---------- Run Section -----------

thermo 1000
run_style verlet
timestep 0.005
```

```
dielectric 0.333

restart 50000 brush.restart

#SIMULATION BOX FIXES

group substrates type 1
group bot_substr id <= 81
group top_substr subtract substrates bot_substr
group polymers type 2
group ctr_ions type 3
group salt subtract all substrates polymers ctr_ions
group dump_group subtract all top_substr
fix 1 substrates setforce 0.0 0.0 0.0
group not_substr subtract all substrates
fix wall1 not_substr wall/lj126 zlo EDGE 0.1 1.0 2.5
fix wall2 not_substr wall/lj126 zhi EDGE 0.1 1.0 2.5

compute real_temp not_substr temp
thermo_style custom step dt c_real_temp press vol etotal ke pe ebond eangle evdwl ecoul
elong

#Minimize the simulation box.
fix poly_hold polymers setforce 0.0 0.0 0.0
minimize 1.0e-6 1.0e-6 2000 2000

unfix poly_hold

#Initial Safe Equilibration to remove bad contacts
velocity not_substr create 1.0 98644713
fix temper not_substr nve/limit 0.1
fix temper2 not_substr langevin 1.0 1.0 100.0 986537
fix rescale0 not_substr temp/rescale 2 1.0 1.0 0.2 1.0
dump 1 dump_group custom 100000 equil.trj id type x y z
run 2000000
unfix rescale0
unfix temper2
unfix temper
undump 1

#Run NVT Sampling
fix 11 not_substr nve
fix 3 not_substr langevin 1.0 1.0 100.0 67016776
dump 2 polymers custom 100000 polymers.trj id type q xu yu zu
dump 55 polymers custom 100000 poly_wrap.trj id type q x y z
```

```
dump 3 ctr_ions custom 100000 ctrions.trj id type q x y z
dump 4 salt custom 100000 salt.trj id type q x y z
run 5000000
unfix 3
unfix 11
undump 2
undump 55
undump 3
undump 4
```